DOI: 10.1002/ejic.200700863

The Oriented Self-Assembly of Magnetic Fe_3O_4 Nanoparticles into Monodisperse Microspheres and Their Use as Substrates in the Formation of Fe_3O_4 Nanorods

Guangcheng Xi,*[a] Chao Wang,[a] and Xing Wang[a]

Keywords: Iron oxides / Magnetic nanocrystals / Crystal growth / Nanorods / Self-assembly

We describe a facile solvothermal route for the large-scale preparation of ferromagnetic Fe_3O_4 sub-micrometer spheres and nanorods by using $FeCl_3$ as the iron source, oleic acid as the surfactant, and ethylene glycol as the reducing agent and solvent. The as-synthesized Fe_3O_4 microspheres are composed of a mess of Fe_3O_4 nanoparticles with a size of 10 nm and have nearly monodisperse diameters that can be controlled in the range 100–410 nm. HRTEM images and SAED patterns show that these microspheres present a "single-crystalline" nature, which can be attributed to the highly oriented assembly of the small Fe_3O_4 nanoparticles. Interestingly, by using the pre-synthesized Fe_3O_4 microspheres as the growth substrate, single-crystalline Fe_3O_4 nanorods can be formed on the surfaces of the microspheres. These nanorods are about 7–20 nm in diameter and 120–400 nm in length, and have smooth surfaces. The formation mechanisms of the Fe_3O_4 microspheres and nanorods have been investigated and discussed. Furthermore, the magnetic properties of the as-synthesized microspheres and nanorods have also been investigated and the magnetization saturation values are 74.6 and 92.3 emu/g, respectively.

Introduction

Nanocrystalline materials have attracted a great deal of attention from researchers in various areas because of both their fundamental size-dependent properties and their many important technological applications. Intensive research has been focused on the synthesis of well-defined uniformly sized nanocrystals in order to identify their size-dependent properties. The size of certain monodisperse particles has been demonstrated to affect their physical and chemical properties, which provide a rational route by which their electronic, optical, and magnetic properties can be tailored.[1–6] The self-assembly of uniform nanoparticles into well-defined two- or three-dimensional superstructures has recently attracted rapidly growing interest owing to their important applications in nanoelectronics, magnetics, optoelectronics, photonics, heterogeneous catalysis, and so forth. More importantly, it allows the exploration of the collective properties of assemblies of particles. Various synthetic methods have been developed to fabricate superstructures composed of nanoparticles.[7–13] For example, monodisperse spherelike semiconductors with micrometer diameters with novel optical, electronic, and photoelectronic properties have been prepared recently.[14]

As a type of important functional material, magnetic nanocrystals have been one of the most-intensively studied owing to their broad applications, for example, in protein separation,[15] as magnetic carriers for drug targeting,[16] in magnetic resonance imaging,[17] and as ultra-high-density magnetic storage media.[18] Among magnetic particles, iron oxides (such as γ-Fe_2O_3 and Fe_3O_4) have been extensively investigated. Monodisperse Fe_3O_4 and γ-Fe_2O_3 nanocrystals with controlled size have been successfully synthesized by various methods. Some of the synthetic routes reported previously in the literature are summarized in Table 1.

Although the approaches to monodisperse iron oxides nanocrystals with diameters below 20 nm have been reported, the synthetic strategies for self-assembled iron oxide superstructures have not attracted enough attention to date. Recently, Shi and co-workers successfully synthesized Fe_3O_4 porous nanospheres with sizes in the range 50–100 nm through a polyol reduction process.[24] These porous nanospheres are composed of a mess of Fe_3O_4 nanoparticles with a size of 5 nm. In contrast to the random aggregation structures of traditional nanoparticle assemblies,[25] these porous Fe_3O_4 nanospheres present an unusual highly oriented attachment structure and display a "single-crystalline"-featured (selected area electron diffraction) SAED pattern. Room-temperature magnetic measurements indicate that the magnetic saturation value for these Fe_3O_4 porous nanospheres is higher than that for the monodisperse Fe_3O_4 nanoparticles with sizes in the range 4–6 nm[26] and lower than that for the single-crystalline Fe_3O_4 sub-micro-

[a] National Nanomaterials Inspection and Research Center, Chinese Academy of Inspection and Quarantine,
Beijing 100025 P. R. China
E-mail: xgch001@mail.ustc.edu.cn
Fax: +86-010-85772625

Table 1. Some synthetic routes towards the preparation of iron oxide nanoparticles reported previously.

	Authors	Material	Reaction Route	Reference
1	A. P. Alivisatos et al.	γ-Fe_2O_3 nanocrystals	thermal decomposition of an iron cupferron complex in octylamine	[19]
2	S. Sun et al.	Fe_3O_4 nanocrystals	high-temperature solution phase reaction of iron(III) acetylacetonate in the presence of oleic acid and oleylamine	[20]
3	V. L. Colvin et al.	Fe_3O_4 nanocrystals	pyrolysis of iron carboxylate salts	[21]
4	T. Hyeon et al.	γ-Fe_2O_3 nanocrystals	thermal decomposition of $Fe(CO)_5$ in oleic acid, trimethylamine oxide, and octyl ether	[22]
5	G. Markovich et al.	Fe_3O_4 nanocrystals	aqueous ammonia reaction with an aqueous solution containing $FeCl_3$ and $FeCl_2$	[23]

meter spheres.[27] These results show that the magnetic properties of Fe_3O_4 nanocrystals are strongly affected not only by their size but also by their attachment structures. Therefore, it is very important to find practical synthetic methods for the size-controlled preparation of Fe_3O_4 nanoparticle assemblies with highly oriented attachment structures. However, to the best of our knowledge, the synthesis of monodisperse sub-micrometer Fe_3O_4 spheres by oriented attachment of small nanoparticles has not been reported until now, which limits the exploration of the collective properties of assemblies of particles.

In this paper, we describe a facile solvothermal route for the size-controlled preparation of sub-micrometer Fe_3O_4 spheres that are ferromagnetic and that may find wide applications in biomedicine and biotechnology. The present approach involves the formation of small magnetic nanoparticles and the subsequent oriented assembly of the nanoparticles to form microspheres with a remarkable "single crystalline" feature. The ferromagnetic microspheres have monodisperse diameters that can be controlled in the range 100–410 nm. Furthermore, the experimental results demonstrate that the spherical Fe_3O_4 aggregates could serve as substrates to grow Fe_3O_4 nanorods, which provides an alternative method for the preparation of Fe_3O_4 one-dimensional (1D) nanostructures.

Results and Discussion

Figure 1 shows a typical XRD pattern of the sample prepared at 200 °C after 20 h under solvothermal conditions, which can be indexed to Fe_3O_4 (JCPDS no. 19-629). No other crystalline materials were detected. It is should be noted that γ-Fe_2O_3 (JCPDS no. 39-1346) has a similar XRD pattern to that of Fe_3O_4, therefore, the XRD patterns could not be used to exactly distinguish the two materials.[28] Recent studies demonstrated that Raman spectroscopy could be an effective method to distinguish iron oxides with different structural phases.[29] For Fe_3O_4 nanocrystals, the spectrum has a main band centered at 668 cm^{-1} (A_{1g}), while the spectrum for γ-Fe_2O_3 nanocrystals show several bands around 700, 500, and 350 cm^{-1}. The Raman spectrum of the sample is shown as curve a in Figure 2. There is a main and strong peak centered at 667 cm^{-1} and two low-strength peaks centered at 527 and 309 cm^{-1}. In comparison, the Raman spectrum of commercial γ-Fe_2O_3 powders is shown as curve b in Figure 2; three main peaks in the range of 200–800 cm^{-1} are shown. Compared with the strong peak in curve b, the two low-strength peaks in curve a are relatively weak. Recently, Shebanova et al. reported that Fe_3O_4 nanocrystals could be transformed into γ-Fe_2O_3 nanocrystals by laser irradiation after a short time. Their results also indicated that if the irradiation time was long enough, Fe_3O_4 would transform completely into α-Fe_2O_3.[29] These phenomena have also been observed by Pinna et al.[28a] Therefore, the formation of the two low-strength peaks in our Raman spectrum (curve a) probably arise as a result of laser irradiation during the measurement. It is therefore rational to deduce that the sample is

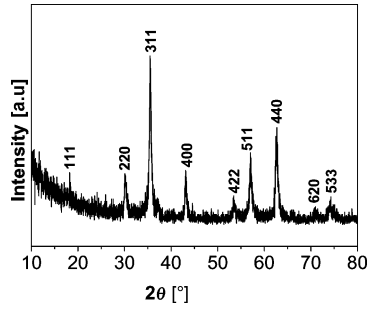

Figure 1. XRD pattern of the as-synthesized Fe_3O_4 microspheres.

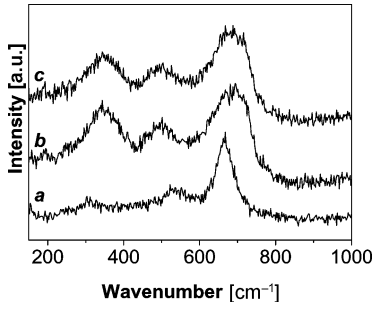

Figure 2. Raman spectra of : (a) the as-synthesized Fe_3O_4 microspheres, (b) the commercial γ-Fe_2O_3 powders, (c) the Fe_3O_4 microspheres irradiated over a long time.

composed of Fe_3O_4 nanocrystals. Furthermore, when the irradiation time was increased to 30 min, the two low-strength peaks evolved into strong peaks, which clearly demonstrates the transformation process from Fe_3O_4 nanocrystals into Fe_2O_3. XPS was used to further detect the purity of the sample. Figure 3 shows the spectrum in which binding energies of 710.4 and 724.2 eV, corresponding to $Fe2p_{3/2}$ and $Fe2p_{1/2}$, respectively, can be deduced. From the combined XRD, Raman spectroscopic, and XPS analyses, it can be concluded that highly crystalline Fe_3O_4 has been synthesized by the present route.

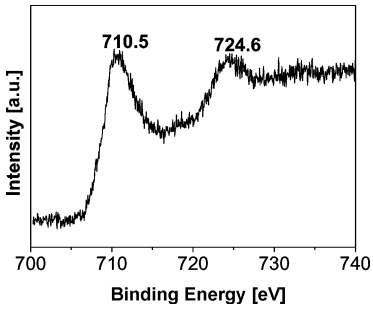

Figure 3. XPS spectrum of the as-synthesized Fe_3O_4 microspheres.

The size and shape of the products were examined by field-emission scanning electron microscopy (FSEM) and transmission electron microscopy (TEM). Figure 4a shows a low-magnification FSEM image of the sample. It can be seen that the sample is composed of densely packed spherical particles with a relatively uniform diameter of about 315 nm. The FSEM image at high magnification shows that the individual spheres are composed of irregular nanoparticles with a size of 10 nm (Figure 4b). Figure 4c shows a typical TEM image of the as-prepared Fe_3O_4 microspheres and shows that the microspheres are composed of a large quantity of small nanoparticles. Interestingly, SAED patterns of the microspheres show bright and regularly arrayed diffractive dots, which indicate that these microspheres were formed by the oriented assembly of the small Fe_3O_4 nanoparticles, i.e. these microspheres are "single crystalline". A typical HRTEM image recorded from the edge of an aggregated sphere is shown in Figure 4d, which clearly demonstrates that all the primary nanoparticles have parallel lattice fringes. On the basis of the above analyses, it can be concluded that the spherelike aggregates are fabricated by oriented assembly.

To understand the formation mechanism of the Fe_3O_4 microspheres under the present experimental conditions, we surveyed the growth process by analyzing the samples at different growth stages. Figure 5 shows the TEM images of three intermediary samples that were taken at different stages of the solvothermal reaction: 2, 8, 15, and 20 h. After 2 h of reaction, the initial product formed was Fe_3O_4 nanoparticles with a size of about 10 nm (Figure 5a), which did not self assemble into aggregated particles. After 8 h, small aggregated particles formed from the self assembly of these nanoparticles; however, the small aggregated particles do not have a distinct (Figure 5b). After 15 h, most of the

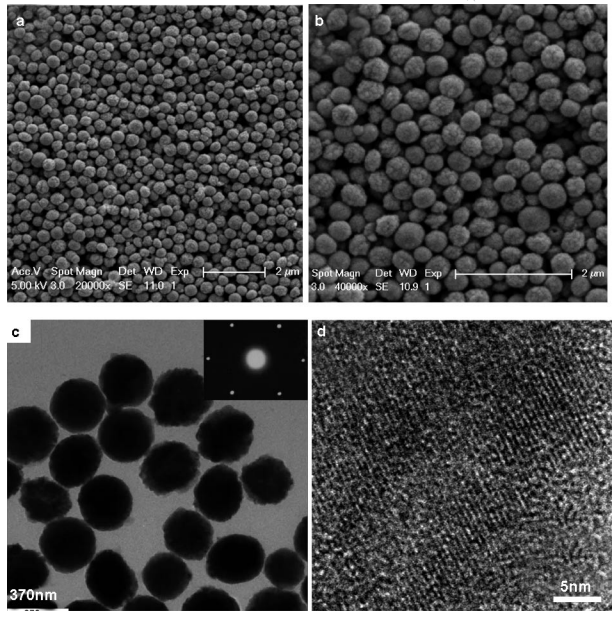

Figure 4. (a, b) Low- and high-magnification FSEM images of the as-synthesized Fe_3O_4 microspheres, respectively (c) TEM image of the Fe_3O_4 microspheres (inset: SAED pattern of one single sphere), (d) HRTEM image of the Fe_3O_4 microspheres.

nanoparticles self assembled into spherelike particles; however, the size distribution of the spherelike congeries is broad (Figure 5c). Finally, as the solvothermal reaction was allowed to proceed for a long time (20 h), the almost complete formation of uniform microspheres was observed with almost no Fe_3O_4 nanoparticles (Figure 5d). From the above experimental observations, we believe that the formation of the Fe_3O_4 microspheres can be rationally expressed as an oriented assembled mechanism. Firstly, when the reduction

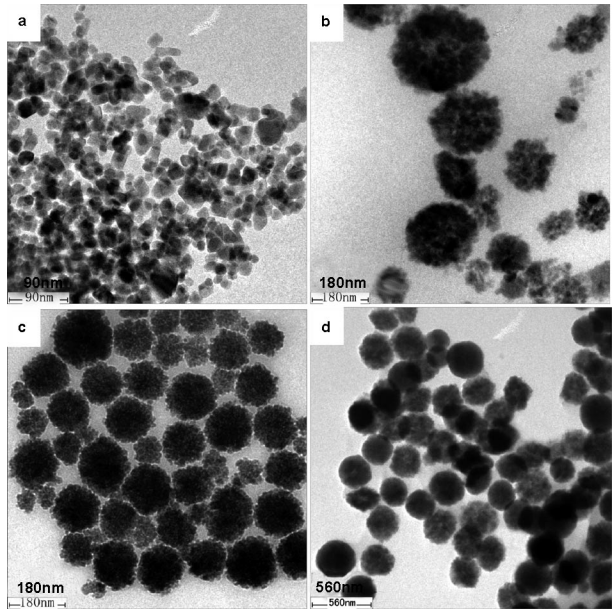

Figure 5. TEM images of the Fe_3O_4 microspheres formed at different reaction times while all other reaction parameters remain unchanged: (a) 2 h, (b) 8 h, (c) 15 h, (d) 20 h.

reaction was carried out in the solvothermal system at 200 °C, it directly gave Fe_3O_4 nanocrystals, which were formed in solution by the reduction of $FeCl_3$ with ethylene glycol. To reduce the high surface energy, these initially formed Fe_3O_4 nanoparticles tend to form aggregates by oriented assembly. This phenomenon is similar to that observed by Shi et al.,[24] but in contrast to that observed by Li et al.[27] Shi et al. synthesized porous Fe_3O_4 aggregated spheres with diameters of 50–100 nm by using iron acetylacetonate as the iron source, ethylene glycol as the reducing agent, and poly(vinylpyrrolidone) (PVP) as the surfactant. In contrast, Li et al. prepared single-crystalline Fe_3O_4 microspheres by using $FeCl_3$ as the iron source and ethylene glycol as the reducing agent; no surfactant was added. Therefore, it is rational to conclude that the surfactant plays an important role in the formation of aggregated microspheres of Fe_3O_4. In our experiments, oleic acid was used as the surfactant, and it may have had a similar effect to that of PVP reported by Shi et al. During the reaction process, oleic acid molecules cover the surfaces of the initially generated Fe_3O_4 nanoparticles; this stabilizes the nanoparticles and effectively confines their random Brownian movements and various rotations. As a result, highly ordered aggregates are formed by oriented assembly of the Fe_3O_4 nanoparticles that are coated with oleic acid molecules. By keeping the other reaction parameters unchanged, the control experiments demonstrated that rhombic Fe_3O_4 nanoparticles are the products when no oleic acid was added into the reaction mixture (Figure 6). This demonstrates that oleic acid plays an important role in the formation of the assembled microspheres. The exact mechanism for the formation of the assembled Fe_3O_4 microspheres by the method presented herein needs further probing.

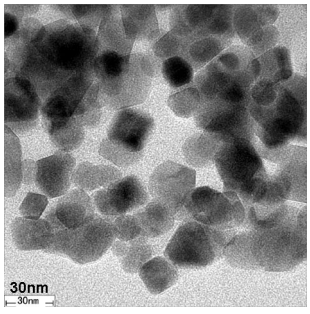

Figure 6. TEM image of the sample prepared under a similar synthetic route, whithout the addition of oleic acid to the reaction mixture.

Furthermore, the diameters of the Fe_3O_4 microspheres are influenced by the concentration of the starting materials. For example, by keeping other reaction parameters unchanged and as the precursor concentration of Fe^{3+} was increased from 30 to 57, 139, 173, and 243 mM, the average diameter of the resulting microspheres increased gradually. The TEM images and histograms of the particle size distribution are presented in Figure 7.

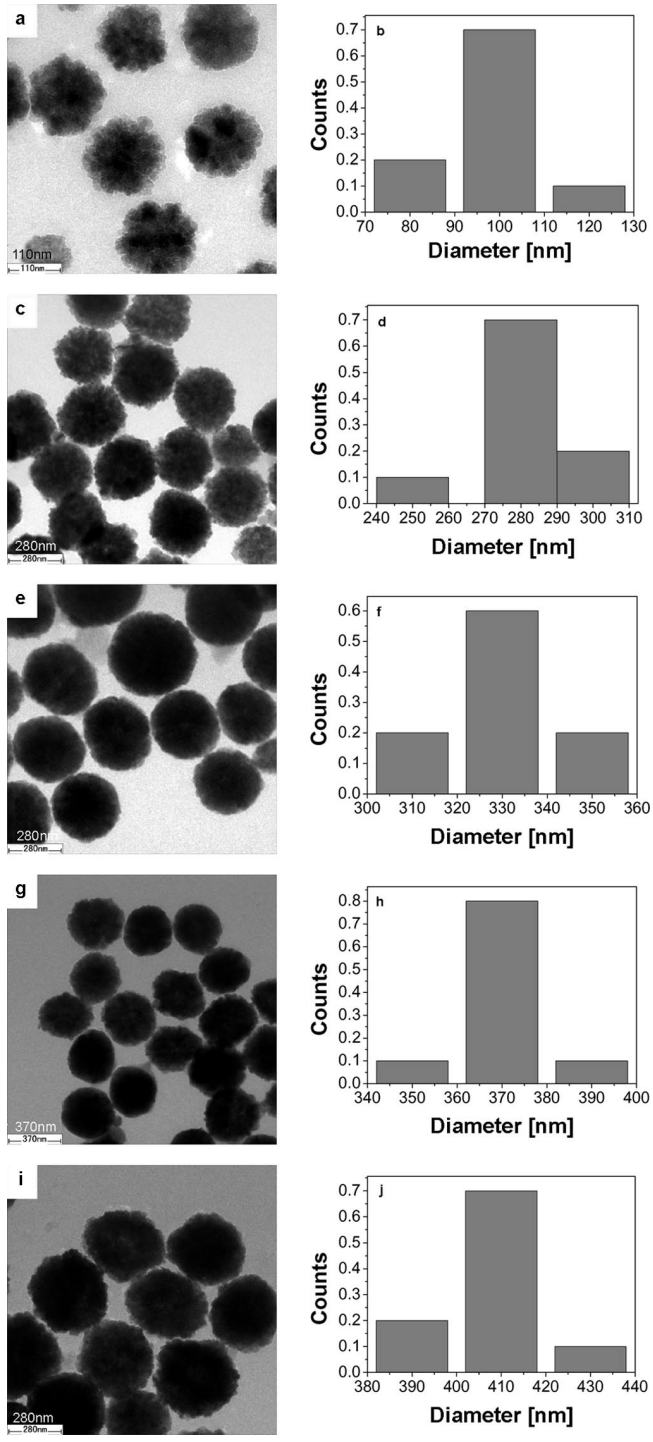

Figure 7. TEM images of Fe_3O_4 microspheres synthesized with different initial concentrations of Fe^{3+} while all other reaction parameters remain unchanged: (a) 30 mM, (c) 57 mM, (e) 139 mM, (g) 173 mM, (i) 243 mM. Histograms of the size distributions for each corresponding TEM image are also shown (b, d, f, h, j, respectively).

Interestingly, by using these Fe_3O_4 microspheres as growth substrates, Fe_3O_4 nanorods could be formed at the surfaces of the microspheres. Figure 8a, b shows the low- and high-magnification FSEM image of the Fe_3O_4 nanorods, respectively, which reveal that the nanorods are

straight and aligned at the surface of the microsphere. The experimental results indicate that the nanorods are loosely attached to the surfaces of the microspheres, and they could be collected by ultrasonic treatment. The TEM image shows that the free nanorods are about 7–20 nm in diameter and 120–400 nm in length and that the surfaces of the nanorods are very smooth (Figure 8c). The HRTEM image of one single nanorod shows that the nanorod is a structurally uniform single crystal. The two spacings of 0.29 nm are consistent with the planes (022) and (202), which suggests that the growth direction of the nanorod is [110]. The SAED pattern of the nanorod (inset in Figure 8d) further demonstrates its single-crystalline nature. EDS analysis was performed on an isolated single rod, with a local probe diameter of 25 nm. Figure 8e shows a representative EDS spectrum of the central part of a rod. Iron and oxide peaks can clearly be observed in this spectrum. The Cu and C peaks arise from the copper TEM grid used in the measurements. Figure 9 shows a histogram with the size distribution of the as-synthesized Fe_3O_4 nanorods.

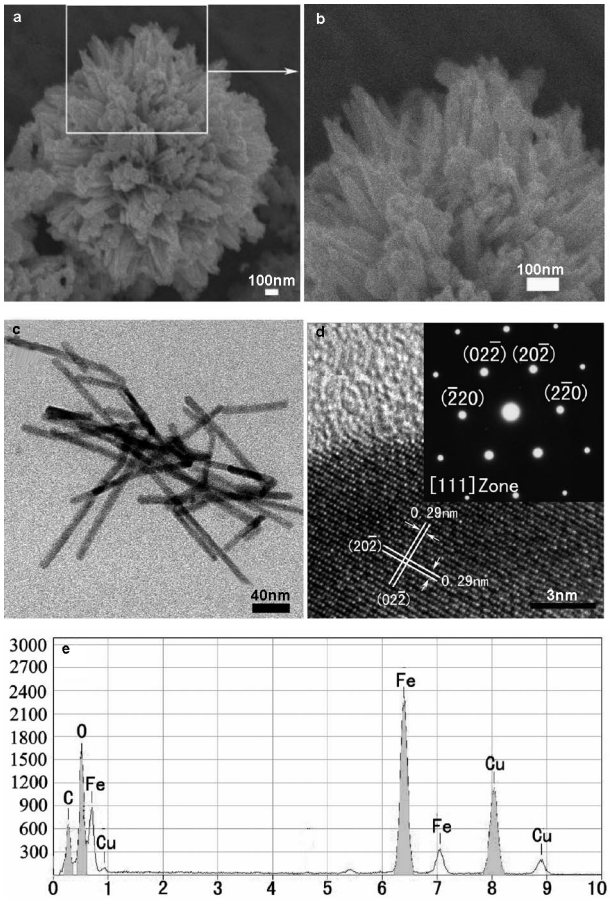

Figure 8. (a, b) Low- and high-magnification FSEM images of the as-synthesized Fe_3O_4 nanorods, (c) TEM image of the Fe_3O_4 nanorods, (d) HRTEM image of one single Fe_3O_4 nanorod (inset: the corresponding SAED pattern), (e) EDS spectrum of one single Fe_3O_4 nanorod.

To understand the growth process of Fe_3O_4 nanorods prepared in a solvothermal system, the Fe_3O_4 nanostructures were characterized at various stages of the growth process by FSEM. Figure 10a–h shows images of the samples that were taken from the reaction mixture after an aging time of 3, 6, 9, and 12 h at 200 °C. After 3 h of reaction, many small Fe_3O_4 protuberant arrays were found growing upright from the surface of the microspheres (Figure 10a, b). After 6 h, some of the small protuberances were transformed into short nanorods (Figure 10c, d). After 9 h, most of the small protuberances were transformed into short nanorods (Figure 10e, f). Finally, as the reaction was allowed to proceed for a long time (12 h), the short nanorods evolved into relatively longer nanorods (Figure 10g, h). Although the exact formation mechanism of the nanorods is unclear at this moment, we believe that these pre-synthesized Fe_3O_4 microspheres play an important role during the growth of the nanorods. It should be noted that there are many small Fe_3O_4 nanoparticles on the surfaces of the microspheres, which offer a large quantity of nucleation sites in the nonaqueous system. When Fe^{3+} iron atoms are reduced to Fe_3O_4 by ethylene glycol, the newly formed Fe_3O_4 clusters tend to nucleate and grow bigger on the nucleation sites. Therefore, Fe_3O_4 nanorods grow epitaxially on the surfaces, as is shown in the images. The process for the transition from microspheres to nanorods is summarized in Figure 11.

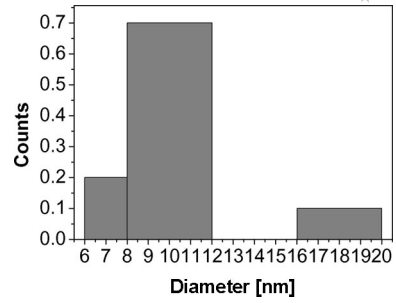

Figure 9. Histogram of the size distribution of the Fe_3O_4 nanorods.

The magnetic properties of the Fe_3O_4 microspheres and nanorods were investigated at room temperature. The magnetic saturation values are 74.6 and 92.3 emu/g for the Fe_3O_4 microspheres and nanorods, respectively (Figure 12). Recently, Shi et al. reported that monodisperse Fe_3O_4 nanoporous spheres composed of nanoparticles with a size of 5 nm were synthesized. The nanoporous spheres are about 50 nm in diameter and show a magnetic saturation value of 42.8 emu/g. The magnetic saturation value of the present Fe_3O_4 microspheres is higher than that of the nanoporous spheres reported by Shi et al. Generally, magnetic Fe_3O_4 nanocrystals show superparamagnetic properties when the nanocrystal size decreases to below 20 nm, i.e. the magnetic saturation value of the nanoparticles increases with an increase in the size of the nanoparticles. Therefore, we believe that the difference in the magnetic saturation value of the present Fe_3O_4 microspheres and that of the nanoporous spheres reported by Shi et al. could rationally be attributed to the different sizes of nanoparticles that make up the spherelike aggregates. Further, the highly oriented self-assembled structure of the Fe_3O_4 microspheres

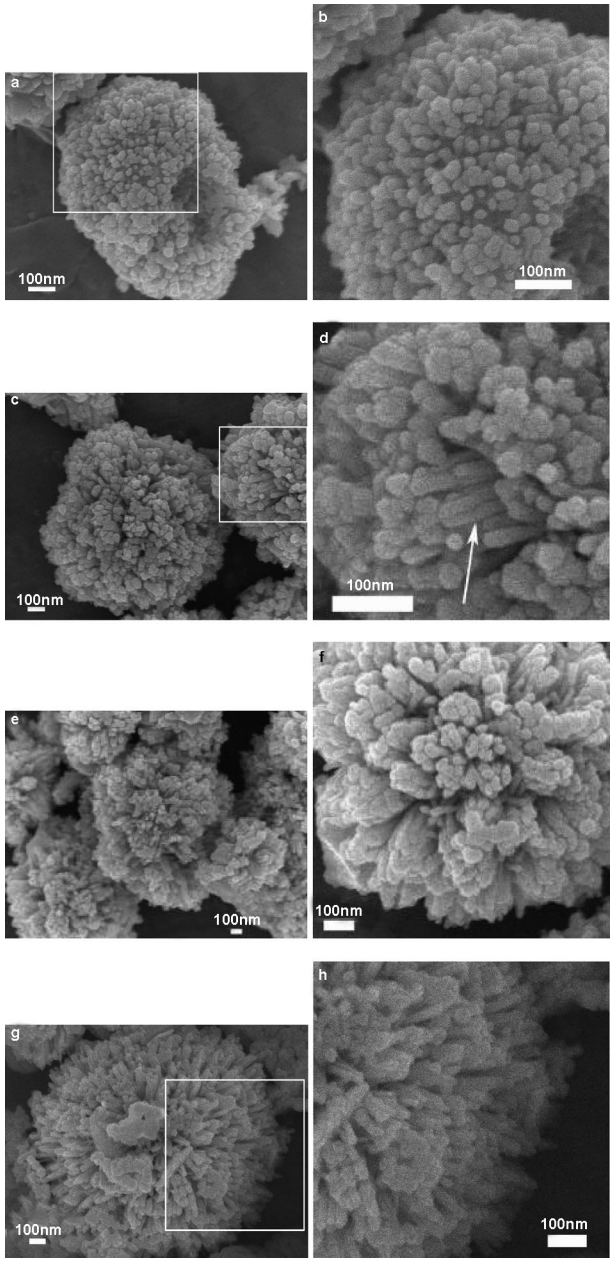

Figure 10. FSEM images of Fe_3O_4 nanorods formed at different reaction times while all other reaction parameters remain unchanged: (a, b) 3 h, (c, d) 6 h, (e, f) 9 h, (g, h) 12 h.

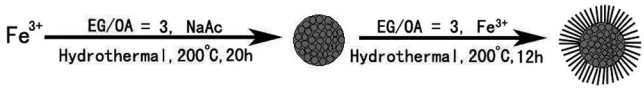

Figure 11. Schematic illustration of the formation of Fe_3O_4 microspheres and nanorods.

may influence the magnetic properties. It should be noted that the magnetic saturation value of the self-assembled Fe_3O_4 microspheres is similar to that of the single-crystalline Fe_3O_4 microspheres reported by Li et al. Since the SAED pattern of the present Fe_3O_4 microspheres displays their "single-crystalline" nature, it is rational to believe that the highly oriented self-assembled structure probably enhances the dipole–dipole interactions between the magnetic nanocrystals. As a result of this effect, the magnetic saturation value of the nanocrystals increases. As for the Fe_3O_4 nanorods, the magnetic saturation value of the nanorods is higher than that of the microspheres, which could be attributed to the larger size of the nanorods.

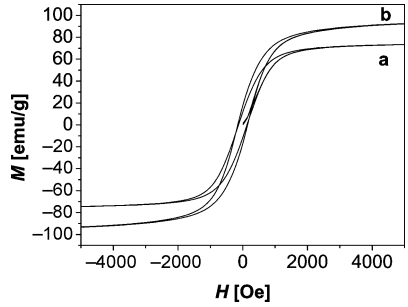

Figure 12. Room-temperature magnetization curves for Fe_3O_4 (a) microspheres, (b) nanorods.

Conclusions

In summary, ferromagnetic Fe_3O_4 sub-micrometer spheres and nanorods were synthesized by using $FeCl_3$ as an iron source, oleic acid as a surfactant, and ethylene glycol as a reduction agent. The as-synthesized Fe_3O_4 microspheres have nearly monodisperse diameters that can be controlled in the range 100–410 nm. The HRTEM images and SAED patterns show that these microspheres present a "single-crystalline" nature, which can be attributed to the highly oriented self assembly of the small Fe_3O_4 nanoparticles. Furthermore, by using the pre-synthesized Fe_3O_4 microspheres as the growth substrate, single-crystalline Fe_3O_4 nanorods can be formed on the surfaces of the microspheres, which provides an alternative method to the preparation of Fe_3O_4 1D nanostructures. The magnetic properties of the as-synthesized microspheres and nanorods were also investigated and the magnetization saturation values are 74.6 and 92.3 emu/g, respectively.

Experimental Section

Materials: All reagents used were analytically pure, and were purchased from Shanghai Chemical Reagent Company and were used without further purification.

Synthesis of Fe_3O_4 Microspheres: In a typical synthetic process, $FeCl_3 \cdot 3H_2O$ (1 g), sodium acetate (NaAc, 3 g), oleic acid (10 mL), and ethylene glycol (30 mL) were placed in a three-necked flask. The reaction mixture was heated to 50 °C for 20 min, and a clear saffron solution formed. The obtained solution was then transferred to a Teflon-lined autoclave with a 60-mL capacity. The autoclave was sealed, heated to 200 °C for 20 h, and then cooled to room temperature. The resulting black precipitate was retrieved by centrifugation, washed several times with distilled water and absolute ethanol, and dried under vacuum at 50 °C for 5 h.

Synthesis of Fe_3O_4 Nanorods: The pre-synthesized Fe_3O_4 microspheres, $FeCl_3 \cdot 3H_2O$ (0.5 g), NaAc (3 g), oleic acid (10 mL), and

ethylene glycol (30 mL) were placed in a three-necked flask and stirred vigorously to form a black suspension. The obtained black suspension was then transferred to a Teflon-lined autoclave with a 60-mL capacity. The autoclave was sealed, heated to 200 °C for 12 h, and then cooled to room temperature. The resulting black precipitate was retrieved by centrifugation, washed several times with distilled water and absolute ethanol, and dried under vacuum at 50 °C for 5 h.

Characterization: XRD patterns of the products were recorded on a Rigaku (Japan) D/max-γA X-ray diffractometer equipped with graphite monochromatized Cu-K_α radiation (λ = 1.54178 Å). FSEM images of the products were recorded on a JEOL-6300F microscope. TEM images, SAED patterns, and HRTEM images were recorded on a JEOL 2010 electron microscope. The Raman spectra were recorded at room temperature on a Spex 1403 Raman spectrometer with an argon-ion laser at an excitation wavelength of 514.5 nm. The X-ray photoelectron spectra were performed on a VGESCALAB MKII X-ray photoelectron spectrometer, by using non-monochromatized Mg-K_α radiation as the excitation source. The magnetic measurements were performed with a superconducting quantum interference device (SQUID) magnetometer (Quantum Design MPMS XL-7).

Acknowledgments

We acknowledge the Dean Foundation of Chinese Academy of Inspection and Quarantine (2007JK014).

[1] a) X. G. Peng, L. Manna, W. D. Yang, J. Wickham, E. Scher, A. Kadavanich, A. P. Alivisatos, *Nature* **2000**, *404*, 59; b) Z. A. Peng, X. G. Peng, *J. Am. Chem. Soc.* **2001**, *123*, 1389; c) X. G. Peng, *Adv. Mater.* **2003**, *15*, 459; d) N. Pradhan, X. G. Peng, *J. Am. Chem. Soc.* **2007**, *129*, 3339.
[2] Y. Huang, X. Duan, C. M. Lieber, *Science* **2001**, *291*, 630.
[3] a) N. R. Jana, L. Gearheart, C. J. Murphy, *Adv. Mater.* **2001**, *13*, 1389; b) K. K. Caswell, C. M. Bender, C. J. Murphy, *Nano Lett.* **2003**, *3*, 667; c) B. D. Busbee, S. O. Obare, C. J. Murphy, *Adv. Mater.* **2003**, *15*, 414; d) T. K. Sau, C. J. Murphy, *J. Am. Chem. Soc.* **2004**, *126*, 8648.
[4] a) Z. Tang, N. A. Kotov, M. Giersig, *Science* **2002**, *297*, 237; b) X. R. Liang, S. S. Tan, Z. Y. Tang, N. A. Kotov, *Langmuir* **2004**, *20*, 1016; c) Z. Tang, Y. Wang, S. Shanbhag, M. Giersig, N. A. Kotov, *J. Am. Chem. Soc.* **2006**, *128*, 6730–6736; d) Z. Tang, N. A. Kotov, *Adv. Mater.* **2005**, *17*, 951.
[5] a) Y. G. Sun, Y. N. Xia, *Science* **2002**, *298*, 2176; b) Y. Lu, Y. D. Yin, B. T. Mayers, Y. N. Xia, *Nano Lett.* **2002**, *2*, 183; c) Y. L. Wang, Y. N. Xia, *Nano Lett.* **2004**, *4*, 2047; d) Y. J. Xiong, J. Y. Chen, B. Wiley, Y. N. Xia, Y. D. Yin, Z. Y. Li, *Nano Lett.* **2005**, *5*, 1237.
[6] a) X. Wang, J. Zhuang, Q. Peng, Y. D. Li, *Nature* **2005**, *437*, 121; b) X. Wang, J. Zhuang, Q. Peng, Y. D. Li, *Adv. Mater.* **2006**, *18*, 2031.
[7] Y. H. Luo, J. G. Huang, L. Ichinose, *J. Am. Chem. Soc.* **2005**, *127*, 8296.
[8] a) F. Kim, S. Kwan, J. Akana, P. D. Yang, *J. Am. Chem. Soc.* **2001**, *123*, 4360; b) P. D. Yang, *Nature* **2003**, *425*, 243.
[9] D. W. Wang, Y. L. Chang, Z. Liu, H. J. Dai, *J. Am. Chem. Soc.* **2005**, *127*, 11871.
[10] B. Liu, H. C. Zeng, *J. Am. Chem. Soc.* **2004**, *126*, 8124.
[11] A. Ghezelbash, B. Koo, B. A. Korgel, *Nano Lett.* **2006**, *6*, 1832.
[12] C. D. Cheng, R. K. Gonela, Q. Gu, D. T. Haynie, *Nano Lett.* **2005**, *5*, 175.
[13] T. K. Sau, C. J. Murphy, *Langmuir* **2005**, *21*, 2923.
[14] a) Q. Peng, Y. J. Dong, Y. D. Li, *Angew. Chem. Int. Ed.* **2003**, *42*, 3027; b) Q. Peng, S. Xu, Z. B. Zhuang, X. Wang, Y. D. Li, *Small* **2005**, *1*, 216.
[15] H. W. Gu, K. Xu, C. J. Xu, B. Xu, *Chem. Commun.* **2006**, 941.
[16] S. Goodwin, C. Peterson, C. Hoh, C. Bittner, *J. Magn. Magn. Mater.* **1999**, *194*, 132.
[17] M. Zhao, L. Josephson, Y. Tang, R. Weissleder, *Angew. Chem. Int. Ed.* **2003**, *42*, 1375.
[18] S. H. Sun, C. B. Murray, D. Weller, L. Folks, A. Moser, *Science* **2000**, *287*, 1989.
[19] J. Rockenberger, E. C. Scher, A. P. Alivisatos, *J. Am. Chem. Soc.* **1999**, *121*, 11595.
[20] S. Sun, H. Zeng, *J. Am. Chem. Soc.* **2002**, *124*, 8204.
[21] W. W. Yu, J. C. Falkner, C. T. Yavuz, V. L. Colvin, *Chem. Commun.* **2004**, 2306.
[22] T. Hyeon, *Chem. Commun.* **2003**, 927.
[23] T. Fried, G. Shemer, G. Markovich, *Adv. Mater.* **2001**, *13*, 1158.
[24] Y. F. Zhu, W. R. Zhao, H. R. Chen, J. L. Shi, *J. Phys. Chem. C* **2007**, *111*, 5281.
[25] a) E. L. Bizdoaca, M. Spasova, M. Farle, M. Hilgendorff, F. Caruso, *J. Magn. Magn. Mater.* **2002**, *240*, 44; b) S. C. Gu, T. Shiratori, M. Konno, *Coll. Pol. Sci.* **2003**, *281*, 1076–1081; c) Q. Z. Wu, H. Q. Cao, S. C. Zhang, X. R. Zhang, D. Rabinovich, *Inorg. Chem.* **2006**, *45*, 7316; d) X. B. Cao, L. Gu, L. Zhuge, W. J. Gao, W. C. Wang, S. F. Wu, *Adv. Funct. Mater.* **2006**, *16*, 896; e) J. C. Bao, Y. Y. Liang, Z. Xu, L. Si, *Adv. Mater.* **2003**, *15*, 1832; f) H. P. Liang, H. M. Zhang, J. S. Hu, Y. G. Guo, L. J. Wan, C. L. Bai, *Angew. Chem. Int. Ed.* **2004**, *43*, 1540.
[26] a) S. H. Yun, B. Y. Sohn, J. C. Jung, W. C. Zin, J. K. Lee, O. Song, *Langmuir* **2005**, *21*, 6548; b) X. Liang, X. Wang, J. Zhuang, Y. T. Chen, D. S. Wang, Y. D. Li, *Adv. Funct. Mater.* **2006**, *16*, 1805; c) Z. Li, Q. Sun, M. Y. Gao, *Angew. Chem. Int. Ed.* **2005**, *44*, 123.
[27] H. Deng, X. L. Li, Q. Peng, X. Wang, J. P. Chen, Y. D. Li, *Angew. Chem. Int. Ed.* **2005**, *44*, 2782.
[28] a) N. Pinna, S. Grancharov, P. Beato, P. Bonville, M. Antonietti, M. Niederberger, *Chem. Mater.* **2005**, *17*, 3044; b) Z. H. Jing, S. H. Wu, *J. Solid State Chem.* **2004**, *177*, 1213.
[29] a) O. Shebanova, P. Lazor, *J. Solid State Chem.* **2003**, *174*, 424; b) O. Shebanova, P. Lazor, *J. Raman Spectrosc.* **2003**, *34*, 845.

Received: August 20, 2007
Published Online: December 17, 2007

